Two-phase PIV to investigate spray/flow interaction in Gasoline Direct injection engine

Julien Lemétayer, Armelle Cessou, Eric Domingues, Bertrand Lecordier, Corine Lacour

Two-phase PIV to investigate spray/flow interaction in Gasoline Direct injection engine

Julien Lemétayer*, Armelle Cessou, Eric Domingues, Bertrand Lecordier, Corine Lacour

CORIA UMR 6614 CNRS – Site Universitaire du Madrillet (BP12), F-76801 Saint Etienne du Rouvray Cedex
*Correspondent author: julien.lemetayer@coria.fr

Abstract This paper focus on the influence of the injection on the internal aerodynamic in an engine. Firstly, velocity measurements have been performed in an optical mono-cylinder engine with fuel injection through a solenoid multi-hole injector using Particle Imaging Velocimetry (PIV) technique. Only gaseous phase is studied in the engine for acquisition timings for which fuel droplets are totally evaporated. Results indicate that the injection impacts the in-cylinder flow by several means. The tumble position and intensity are modified. Injection reduces the cycle-to-cycle variations of the tumble and maintains it around the chamber mid-height until 100 BTDC. The tumble intensity is also almost twice less important with injection. The velocity magnitude is globally lower and less fluctuating during the cycle. The turbulence is also reduced in the presence of the injection and velocity fluctuations are more spatially homogeneous than without injection. Secondly, a two-phase PIV diagnostic is settled in order to enable a simultaneous measurement of the velocities of liquid and gaseous phases when both are present. Validations of the technique are performed in a static chamber with the same injector than for the study on the engine bench. The two phases are separated during the acquisition using fluorescence signal of two different dyes, recorded on two cameras with filters. The use of a second laser is proposed for this diagnostic to enable to adjust two PIV delays to overcome the difference of velocity range between both phases. The gas velocities measurement has been validated. Finally, this paper highlights two points: (1) injection in the engine clearly impacts the stability of the internal aerodynamic; (2) two-phase PIV using dyes succeeds separating phases to provide well-separated instantaneous velocity fields during injection phase.

1. Introduction

Nowadays, injection technologies for gasoline engines turn towards the direct injection. The question is to know if the presence of a spray in the chamber has an effect on the internal aerodynamic stability and its control. Indeed, the control of the in-cylinder flow is necessary since it influences the mixture composition, its ignition and the flame development, which are decisive steps for the combustion efficiency. The direct injection of a high-pressure spray in the cylinder can induce flow perturbations and eventually degrade the internal aerodynamic. We intend to investigate the nature of the impact the injection has regarding the in-cylinder gas flow. In this context, our study intends to bring a better understanding of the modifications induced by the spray on the in-cylinder flow. These flow perturbations can be of different nature such as stabilizing or accelerating for instance. This experimental work is performed on an AVL optical mono-cylinder engine. The global impact of the injection, preferentially after its end, is highlighted to identify the consequences of the presence of a spray. A first estimation of the spray impact on the internal flow has been performed using the Particle Imaging Velocimetry (PIV) diagnostic restricted to acquisition timings for which fuel droplets are totally evaporated. Then, in order to go further in the investigation of spray/flow interaction before the complete evaporation of fuel droplets, a two-phase PIV technique, based on fluorescent dyes has to be set-up to overcome the difficulties to investigate crank angles where the two phases are present.

The experimental setup and optical technique for the optical mono-cylinder are firstly presented, followed by a discussion about results managed by PIV technique. After that, the two-phase PIV technique is developed with a presentation of first results obtained by this technique.

2. Experimental setup and optical diagnostic material

In order to evidence the impact of the spray injection on the in-cylinder flow, gas flow velocity measurements have been performed on a mono-cylinder engine with conditions close to those of a real engine. The engine test bench consists in a mono-cylinder GDI engine (AVL) with a displacement volume of 450 cm^3 and a compression ratio of 8.5 and operating up to 3000 rpm. The injection system is a common-rail solenoid multi-hole injector Bosch to ensure a stable injection pressure up to 100 bar. Operating conditions are controlled: rotation speed, air mass flow fuel equivalence ratio, the injection timing and duration.

A Quantel Twin Mini supplying 2×30mJ at a wavelength of 532 nm and a 12 bits Hamamatsu camera with a resolution of 2048×2048 pix^2 has been used. The optical accesses to the combustion chamber were enabled by quartz-glass liner. These accesses enable to get a laser sheet corresponding to the symmetric plane of the combustion chamber which contains the injection plane. This classic PIV setup has been adapted to the constraints of laser diagnostics in optical engine (curved glass window, light reflection…) and specific PIV algorithms (masking technique, image correction…) have been used to take into account the permanently evolution of the investigation domain due to the piston motion and light reflections on metallic and glass parts of the combustion chamber. In this study, the measurements managed with this technique are restricted to acquisition timings without any liquid fuel droplet present. This restriction is due to the high level of light scattering by fuel droplets which prevents from a correct acquisition of the scattering of the gas marker (DEHS oil droplets of around 1 µm). The cameras generally do not have a wide enough dynamic range for avoiding strong CCD saturations which can induce camera damages. In addition, in region where both phases can be recorded simultaneously on the CCD, the separation based on signal intensity of each phase by a post-processing is becoming very tricky because the sizes of smallest fuel droplets and air tracers are very similar (Khalitov et al., 2002).

The measurement campaign is based on several operating conditions corresponding to homogeneous combustion at partial load. The injection timing at 320 BTDC and the fuel equivalence ratio of 1 remain constant values for all measurements. The injection duration is adjusted for the engine rotation speed in order to fulfil the equivalence ratio of 1. Measurements have been performed with engine rotation speed of 3000 rpm and injection pressure of 100 bar with an Indicated Mean Effective Pressure (IMEP) of 7.9 bar. For each operating point, acquisitions with the PIV technique are performed for 4 crank angles: 140 BTDC, 120 BTDC, 100 BTDC and 70 BTDC. The comparison of the measurements with and without injection for these conditions will help understanding the influence of fuel injection on the internal aerodynamic.

3. Results

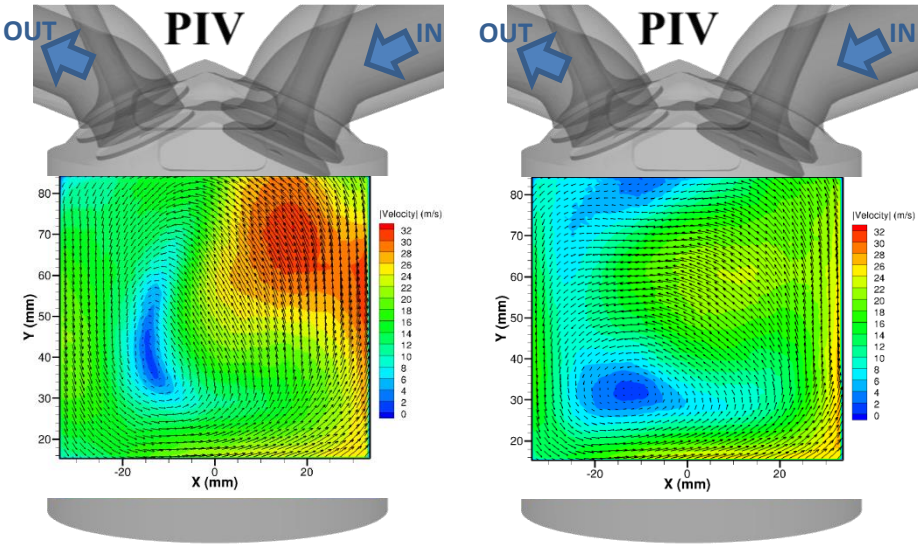

Fig. 1 Measurement configuration of the engine test bench: mean velocity field at 3000 rpm at θ_{acq}=140 BTDC without injection (on left) and with injection (on right)

Figure 1 presents the velocity fields and the velocity amplitude in colour scale for an engine speed of 3000 rpm without (left) and with (right) an injection at 100 bar for an acquisition at 140 BTDC. This figure also enables to place the mean velocity field relatively to the combustion chamber volume. The vertical axis

origin corresponds to the piston surface at the bottom dead centre knowing that the piston stroke is 86 mm. Instantaneous velocity fields are obtained by a PIV post-processing program developed by Lecordier (1997). To reach a non-valid vector rate lower than 5%, a multi-pass subpixel shift correlation algorithm has been necessary. For the first pass, an interrogation windows size of 32×32 pix^2 (1.14×1.14 mm^2) with an overlap of 50% has been used with a correlation based on the Fast Fourier Transformation. Afterward, a Signal to Noise Rate (SNR) of 1.1 and a median filter 3×3 enable to reject most of non-valid vectors. For the next passes, the same parameters than the first pass have been used. Each mean velocity field is obtained thanks to the average of 300 instantaneous velocity fields derived from 300 engine cycles acquired at 10Hz. To avoid statistical errors in the mean calculation, only the valid vectors (not-substituted vectors) are considered. 300 instantaneous velocity fields are necessary for the convergence of the velocity mean standard deviation fields whereas the mean velocity field is converged with about 100 instantaneous fields.

On the Figure 1, meaningful differences can be noted between the cases without and with injection. The tumble centre position is changed and the velocity magnitude is different. These first observations confirm that direct injection impacts significantly the internal aerodynamic in the present configuration.

3.1. Tumble evolution

The kinetic moment or tumble rate is a pertinent parameter for the global investigation of the impact of the spray injection on the large scale structure in the in-cylinder gas flow. In this study, the tumble rate is a non-dimensional number defined by:

$$\tau_z = \frac{\sum_i m_i(\overrightarrow{OM} \wedge \vec{V})\cdot\vec{z}}{\sum_i m_i(\overrightarrow{OM}\cdot\overrightarrow{OM})} \cdot \frac{60}{2\pi N} \qquad (1)$$

In the Equation 1, O represents the reference centre and M the location where the velocity $\vec{V}$ is considered. As local mass variations can be neglected, the mass m_i at location M is simplified in the Equation 1. The definition of the reference point O is not trivial. In this study, the reference is defined as the vortex centre which is detected through the Γ_1 function (Eq. 2) on a circle with a diameter of 10 meshes (11,4 mm).

$$\Gamma_1 = \frac{\sum_i(\overrightarrow{OM} \wedge \vec{V})\cdot\vec{z}}{\sum_i \|\overrightarrow{OM}\| \cdot \|\vec{V}\|} \qquad (2)$$

This criterion is relevant for the location of vortex centre (Graftieaux, 2001). Figure 2 presents the Γ_1 field obtained by the equation (2) in colour scale with its corresponding mean velocity field at 120 BTDC for engine operating at 3000 rpm with an injection. The Γ_1 function detects perfectly the vortex centre on this mean velocity field.

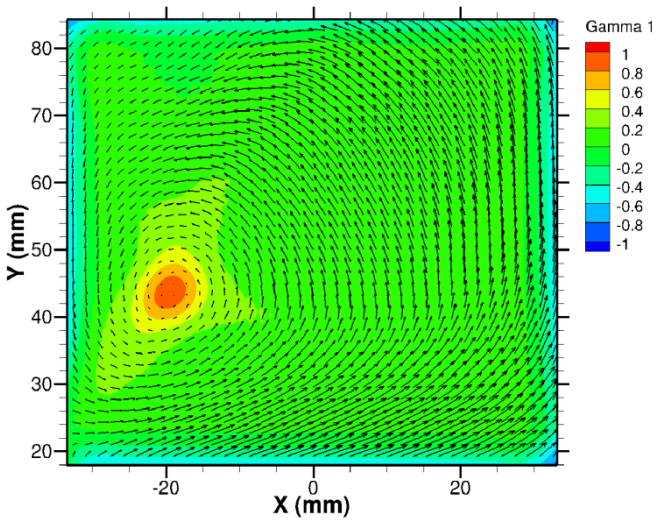

Fig. 2 Mean velocity field (vector) and Γ_1 function (colour scale) at 3000 rpm at θ_{acq}=120 BTDC with injection at 100 bar

The evolution of the tumble centre location in the mean velocity fields has been studied regarding the piston angular position. The Figure 3 presents the location of the tumble centre in the chamber for the several crank angles without and with injection. The Y-axis has been normalised by the gap between the piston and the cylinder head to draw the relative position of the tumble centre in the chamber. Whereas the tumble centre is located in the top part of the chamber after 140 BTDC without injection, it stays in the middle of the chamber till 70 BTDC in the case with injection. Thus, the injection seems to maintain the tumble location near the middle of the chamber and avoid its move towards the top left corner. Only for late acquisition at 70 BTDC, the tumble structure position is equivalent with and without injection.

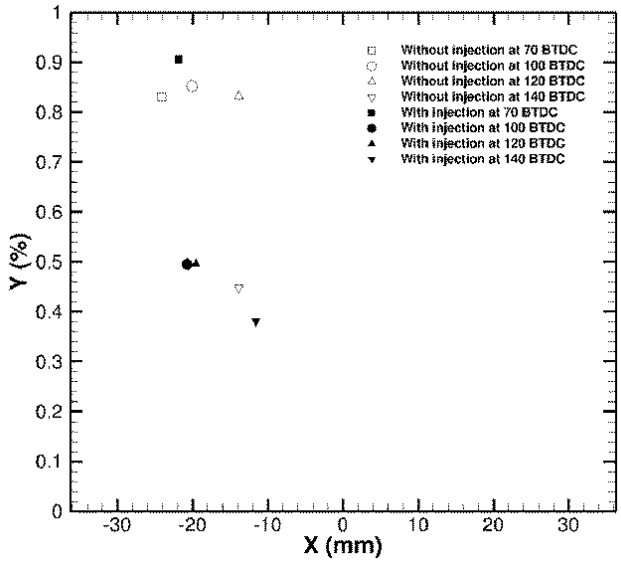

Fig. 3 Evolution of the tumble centre location for the mean velocity fields without (empty symbols) and with (filled symbols) injection

This result shows that the presence of the injection modifies the mean tumble behaviour but certainly also the instantaneous large scale structures position. The dispersion of instantaneous tumble location is investigated after applying a moving average low pass-filter on each instantaneous velocity field. This basic filter is chosen as a preliminary filtering approach which will be improved in future workes. Several cut-off sizes of the filter have been tested and it finally fixed to 15 mm to be around the order of magnitude of the typical integral scale of engine in-cylinder aerodynamic. The tumble location is then easily identified on the instantaneous low-pass filtered velocity fields by means of the Γ_1 function. As on the mean velocity field, his criterion is also applied successfully on the instantaneous velocity fields even if several vortices are present in the flow. Indeed, considering the maximum of the Γ_1 field as the tumble centre, it is correctly determined for most cases. Figure 4 presents the tumble centre locations for acquisitions at 100 BTDC and 140 BTDC with and without injection. On each figure, the tumble centres determined by means of the Γ_1 function for the 300 low-pass filtered instantaneous velocity fields are represented by black spots and the one of the mean velocity field by the red square. The instantaneous velocity fields are affected by the early injection since at 140 BTDC, the tumble centres dispersion is less important with injection than without injection (Figures 4.c and 4.d). The axial dispersion is clearly more pronounced without injection whereas the transverse dispersion seems to be slightly less important without injection. However, this difference seems to weaken during the compression as shown on the Figures 4.a and 4.b.

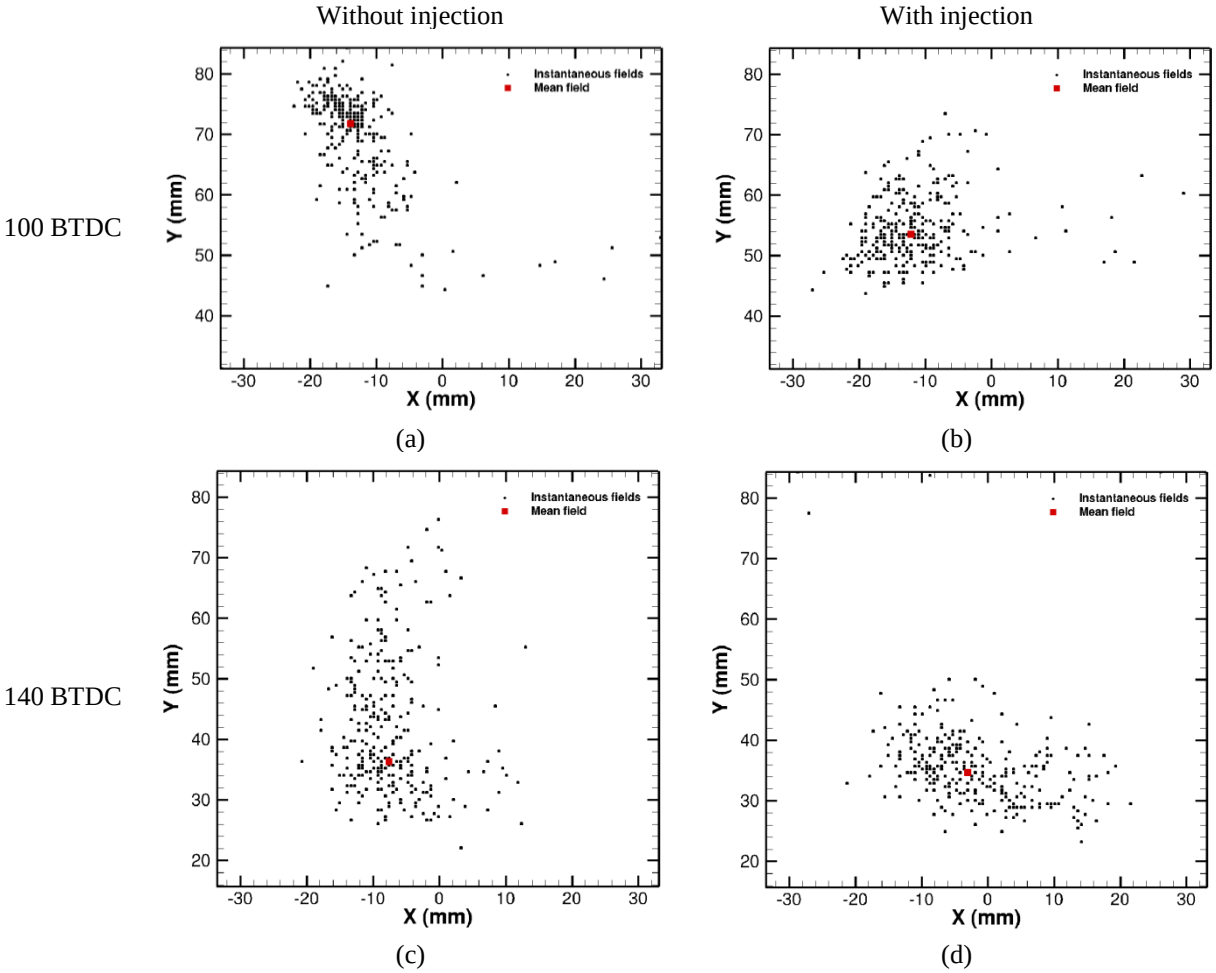

Fig. 4 Location of the tumble centre for the low frequency instantaneous velocity fields (black points) and for the mean velocity field (red square) without (on left) and with (on right) injection

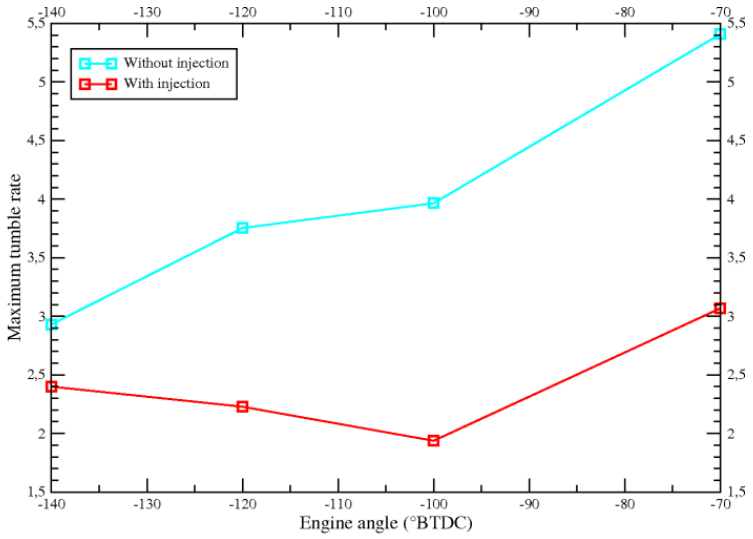

Fig. 5 Maximum of the tumble rate as a function of the crank angle without (blue) and with (red) injection

The tumble intensity is also an interesting parameter since it reveals the angular motion intensity of the gas flow. The Figure 5 represents the evolution of the maximum of the tumble rate according to the crank angle for mean velocity fields at 3000 rpm without and with injection. The tumble rate is obtained as detailed previously (Eq. 1) in a region of 30×30 mm² centred on the tumble centre. The maximum of the tumble rate

is significantly higher without injection and there is nearly a factor 2 between both cases except at 140 BTDC. It appears also that the tumble rate increases continually without injection whereas it slowly decreases until 100 BTDC before rising in the case with injection. The presence of the spray weakens the tumble movement in the chamber and even if the structure seems to form itself again after 100 BTDC, the energy loss is still visible at the end of the compression phase.

3.2. Velocity fluctuations

Previous results have shown that the injection modifies the location and intensity of the tumble, the effect of spray injection on the mean and fluctuations velocity levels will now be investigated. Figure 6 presents the mean velocity fields and the velocity amplitude in colour scale for several crank angles without and with injection. The velocity evolution is different between both cases. Indeed, at 140 BTDC without injection a region of high velocity (around 32 $m.s^{-1}$) exists near the injector zone (top right corner), then the velocity decreases in this region, and finally the flow is accelerated again at 70 BTDC. On the contrary, for injection conditions, no significant variation of the structure of the velocity fields can be noticed and the flow velocities are significantly slower. The velocity difference is particularly visible around the tumble centre since the velocity gradient around it is lower with injection than without injection.

With an injection, the flow dynamics remains similar during the engine cycle and is more spatially homogeneous since velocity gradient are lower. These elements suggest a possible stabilization of the in-cylinder flow thanks to the injection of a spray.

3.3. Turbulence fluctuations

Instantaneous velocity fields have been filtered (as described previously) with the aim of separating large-scale structures contributing mostly in cycle-to-cycle variations and turbulent structures occurring at smaller scales. The mean velocities and mean fluctuating velocities are then obtained from the 300 instantaneous low-frequency velocity fields on the one part and from the 300 instantaneous high-frequency velocity fields on the other part.

Figure 7 presents low-frequency mean fluctuating velocities. It is representative of cycle-to-cycle dispersion of large-scale structures. The fluctuations are significantly lower in the case with injection. This confirms in the present configuration that the early injection of a spray reduces the cyclic dispersion of the large scale structures. It should also be noticed that the maxima of the mean fluctuating velocities do not exactly correspond to the tumble centres (black spots). A region of non-negligible fluctuations is observed in the top part of the investigation area. It is only reduced with injection at 100 BTDC but it is difficult to interpret since the flow velocities have not been measured in the upper part of chamber.

Figure 8 presents high-frequency mean fluctuating velocities. The high velocity zone observed along the top line of the window is attributed to experimental noise. The high-frequency velocities level is near 10 $m.s^{-1}$ near the tumble zone for the case without injection (Figure 8.a), whereas it does not exceed 7 $m.s^{-1}$ and is more spatially homogeneous after the injection (Figure 8.b). At 100 BTDC, the velocity fields are similar except in the top part of the investigation domain (Figures 8.c and 8.d).

Nevertheless, it is premature to conclude about the importance of the cycle-to-cycle variations in the global variations compared to the importance of the turbulent structures. Indeed, the filtering technique applied here is still preliminary and new techniques (POD, wavelet…) have to be considered to go further in a more detailed description of the in-flow and the effect of the injection on the turbulence. It should be also necessary to complete the velocity measurements with and without injection in the upper part of the chamber.

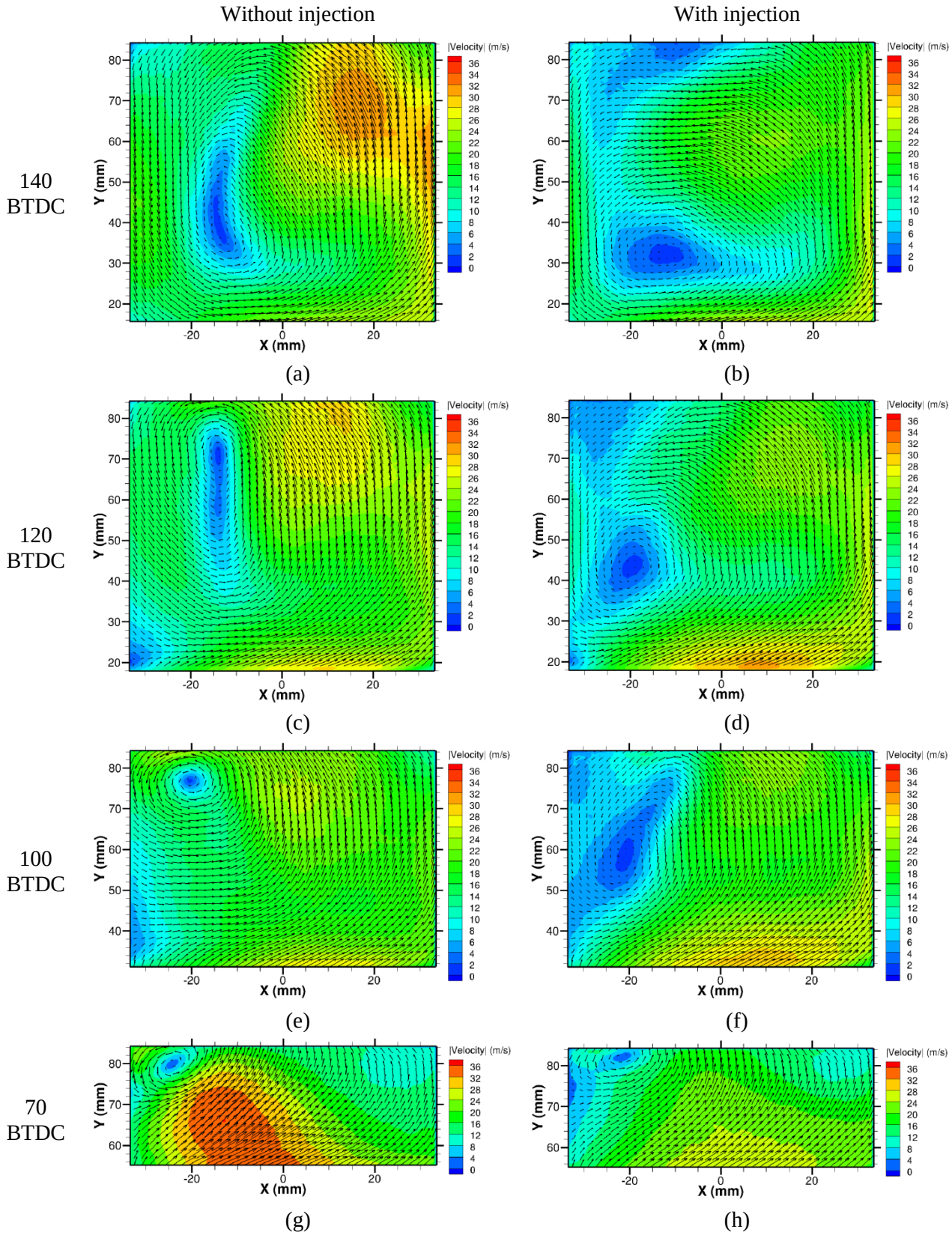

Fig. 6 Mean velocity fields at 3000 rpm for several acquisition timings without (on left) and with (on right) injection

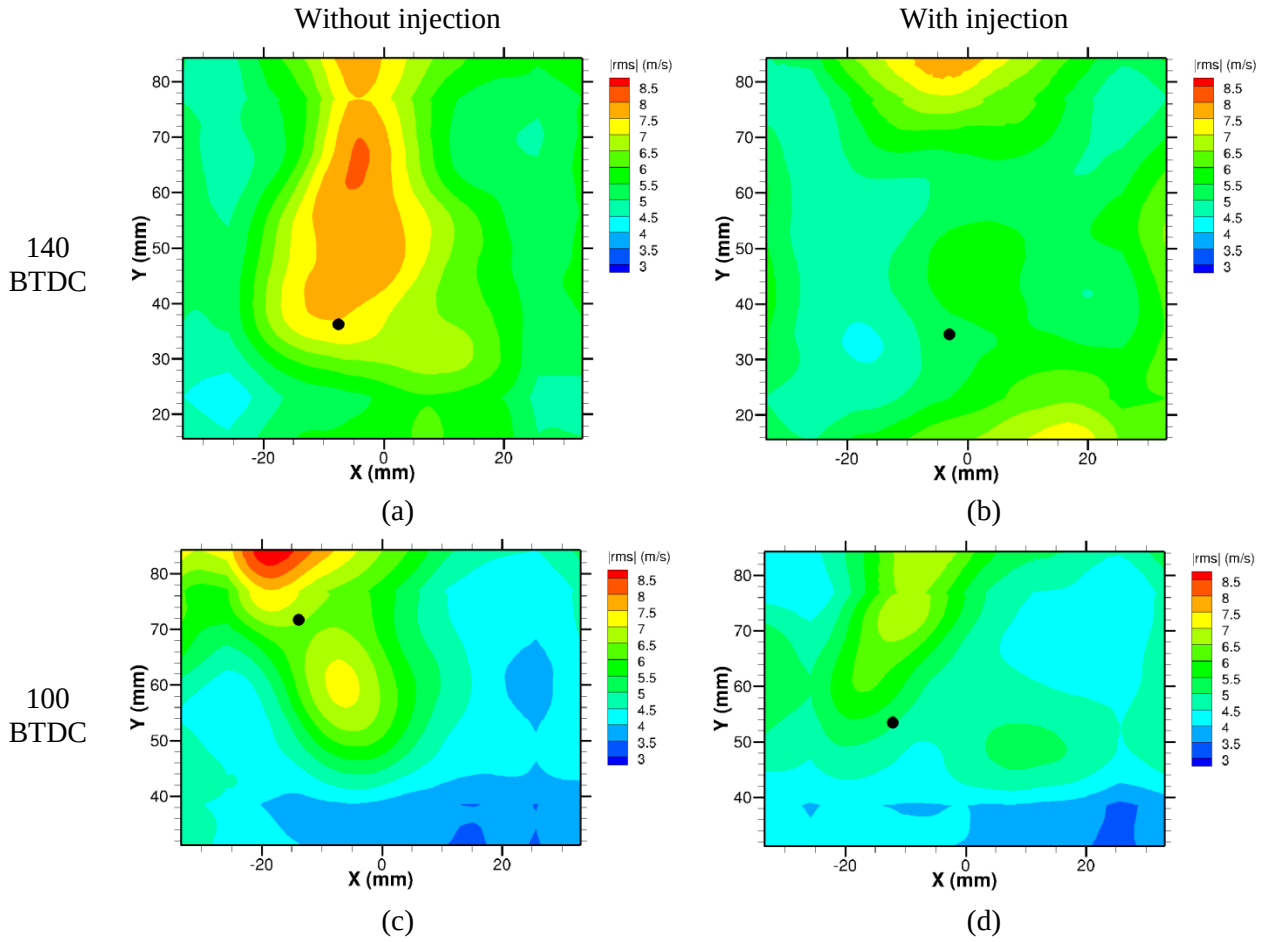

Fig. 7 Low-frequency mean fluctuations fields and tumble centre location (black spot) at 3000 rpm at 140 BTDC and 100 BTDC without (on left) and with (on right) injection

3.4. Conclusion

These first observations confirm that direct injection significantly impacts the internal aerodynamic in the present configuration. To improve our understanding of the coupling between the injection and the gas phase and the momentum transfer between the two phases, it is essential to investigate the in-cylinder aerodynamic for earlier acquisitions timings of the engine cycle when liquid droplets are still present. Therefore, the two-phase flow history will be traced back to completely highlight the causes of the observed phenomena. To achieve this objective, the classic PIV technique is not adequate. Indeed, simultaneous measurements of gas and droplets velocities are needed and so require the discriminating of the signal emitted by each of the two phases. To overcome the limitations of standard PIV to investigate two-phase flow, a PIV approach based on fluorescence emission (Kosiwczuk et al., 2005) will be applied and adapted to enable such a measurement.

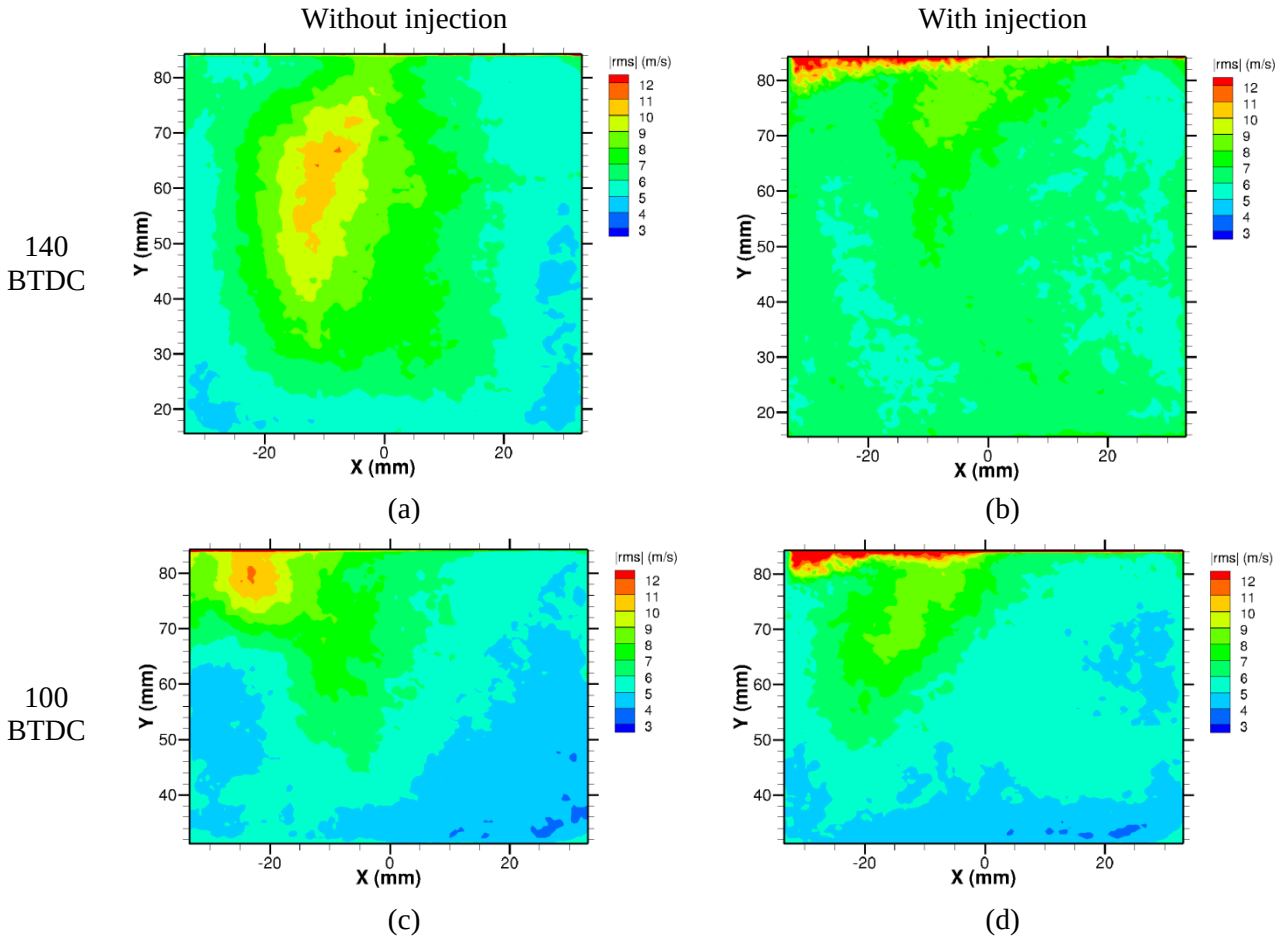

Fig. 8 High-frequency mean fluctuations fields at 3000 rpm at 140 BTDC and 100 BTDC without (on left) and with (on right) injection

4. Two-phase PIV

The two-phase PIV technique is based on the use of two different dyes, with emissions of fluorescence spectrally separated. The phase separation is performed by a detection system consisting of two PIV cameras equipped with adapted pass-band filters. The signals emitted from the gas phase and from the liquid phase are acquired independently by collecting them on separated spectral bands (Figure 9). Velocities of the gas and the liquid phases can thus be acquired simultaneously for engine conditions where the two phases are present, typically early after the start of injection.

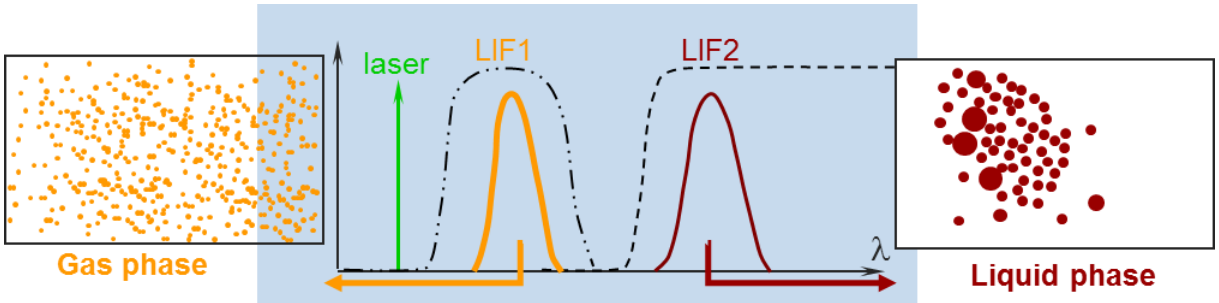

Fig. 9 Principle of two-phase PIV technique

In his study, Kosiwczuk et al. (2005) had already demonstrated the interest of this two-phase PIV technique to investigate air/spray interaction on a fuel injection. For the phase separation, it had been demonstrated that the dyes excitation at 355 nm was more efficient than at 532 nm. However, it had been

shown that the choice of a single PIV laser makes difficult the PIV optimisation for the two phases because in the early stage of injection, the droplets velocities largely exceed the gas phase velocity in such configuration. The fluorescent technique had also been used with an excitation at 532 nm and using the same dye for both phases alternatively in order to measure air entrainment and spray velocity for a diesel application (Hespel et al., 2010). In that case, simultaneous acquisition could not be considered because of the too important difference between velocity ranges of the spray and the gas. This prevents to use only one PIV acquisition delay and obliges to fix different PIV acquisition delays for the gas and for the diesel spray. This difficulty, also noted by Kosiwczuk et al. (2006), leads us to modify the optical diagnostic by using two lasers at different wavelengths (532 nm for the gas and 355 nm for the spray) in order to make optimisation of PIV acquisition delays for each phase possible.

Before performing simultaneous measurements, intensity of the gas phase fluorescence signal has been tested for an ethanol spray in a static chamber since it is the most critical phase to record. Indeed, the fluorescence signal depending on the droplets diameter, the air seeding fluorescence signal is clearly lower than the one of the spray since seeding particles are much smaller than spray droplets. Ethanol is injected at 50 bar with a multi-holes solenoid injector in a gas at rest in a $20\times20\times20cm^3$ chamber. Air is seeded with droplets generated from a solution of Pyrromethene 597 dissolved in DEHS oil at 2 g/L. The diameter of these seeding droplets is about 5 µm and they are excited by a double pulse Nd:YAG laser supplying 2×10mJ at 532 nm. The Mie scattering signal is rejected from the fluorescence signal using a high-pass filter GG570. Figure 10 presents the air seeding particles image in the presence of a spray. It illustrates the rejection of the Mie scattering signal at 532 nm since only a blur zone appears where the spray is located. We think that this blur zone comes from the diffusion of the seeding fluorescence signal by the whole spray. Figure 11 presents a mean velocity field of the gas phase initially at rest, obtained from 30 instantaneous velocity fields. These instantaneous velocity fields have been calculated with a multi-pass algorithm, with an initial window size and iterative windows size of 32×32 pixels ($1.9\times1.9mm^2$) with an overlap of 50%. The mean velocity field clearly indicates that, in the regions where seeding particles overlap with the zone of blur, the velocity vectors are calculated. On the contrary, in the spray core, where no seeding particle is present, the gas velocity cannot be estimated (Figure 11). Gas velocity is determined with accuracy, particularly at the gas/spray interface, showing that the computation is not disturbed by spray droplets. Recirculation structures can be noticed near the spray and different characteristic zones previously defined (Prosperi, 2008) along the spray are observed. The next step to complete this diagnostic is to validate the spray droplets velocity measurement using another dye excited at 355 nm with a second laser in combination with gas velocity measurement with tracers excited at 532 nm.

Thus, this two-phase PIV diagnostic seems very promising to study the effect of the injection on the engine internal aerodynamic. The advantages of this technique are the possibility to simultaneously acquire the instantaneous velocity fields of both phases and the possibility to optimise the PIV acquisition delay for each phase flowing with important velocity differences.

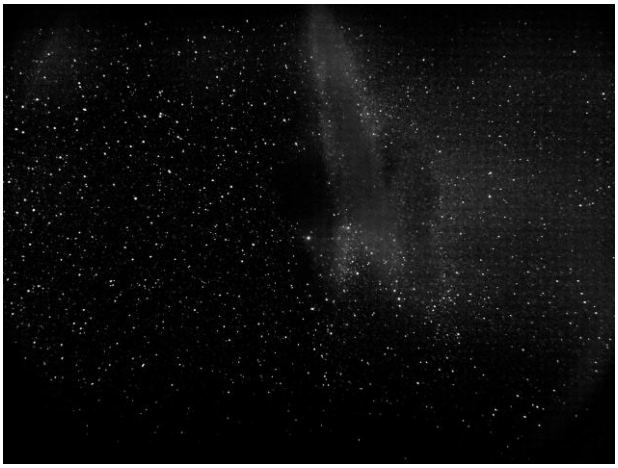

Fig. 10 Particles image in the presence of a spray at 2 ms after the injection start signal

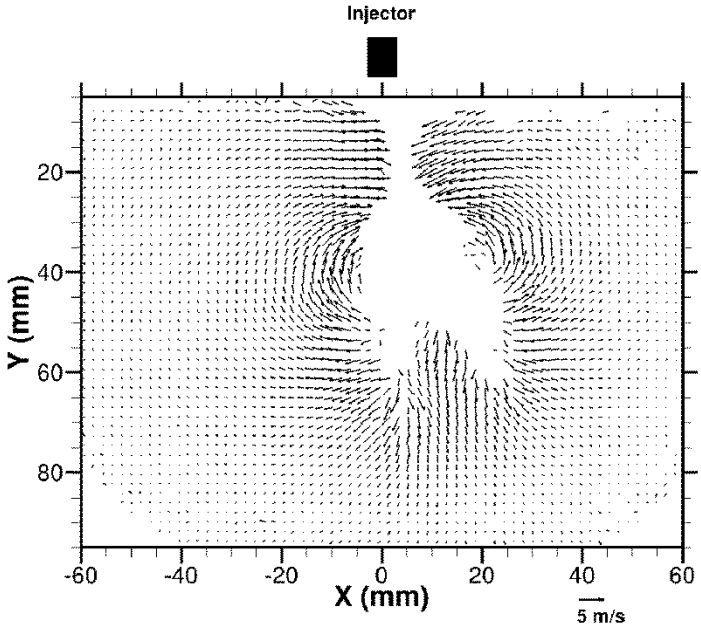

Fig. 11 Gas mean velocity field in the presence of a spray at 2 ms after the injection start signal

5. Conclusion

The main objective of this work is to extend the applicability of two-phase PIV fluorescence technique to investigate two-phase flows in complex environments such as in an engine test bench. It will enable to completely trace back the two-phase flow history in order to understand the dynamic interactions occurring between the two phases. Thus, the impact of the presence of the spray on the stability of the internal aerodynamic will be analysed to help improving its control. The use of the classic PIV technique enables to establish the main modifications induced by the injection on the in-cylinder flow about the tumble location and intensity modifications, the velocity magnitude and the low-frequency and high-frequency fluctuations. The different difficulties and adaptations required to obtained reliable velocity measurement of the two phases are discussed. The combination of two-phase PIV fluorescence technique with the use of a second laser proves to be the right way to overcome the difficulties due to two-phase environment. The interest and the advantages to use such approach to analyse interactions occurring between a fuel spray and the in-cylinder flow in an engine are presented.

Acknowledgments

This work was conducted as part of the ESSENCYELE project (moteur ESSENCe injection directe hYbride Electrique abordabLE), funded by the *Agence De l'Environnement et de la Maîtrise de l'Energie* (ADEME). The material support from the EFS Company is acknowledged.

References

Graftieaux, L.; Michard, M. & Grosjean, N. (2001), 'Combining PIV, POD and vortex identification algorithms for the study of unsteady turbulent swirling flows', Measurement Science and Technology 12(9), 1422.

Hespel, C.; Blaisot, J.B. et al. (2010), 'Influence of Nozzle Geometry on Spray Shape, Particle Size, Spray Velocity and Air Entrainment of High Pressure Diesel Spray', THIESEL 2010 - Conference on Thermo- and Fluid Dynamic Processes in Diesel Engines, 387--399.

Khalitov, D. & Longmire, E. (2002), 'Simultaneous two-phase PIV by two-parameter phase discrimination', *Experiments in Fluids* **32**(2), 252--268.

Kosiwczuk, W.; Cessou, A.; Trinité, M. & Lecordier, B. (2005), 'Simultaneous velocity field measurements in two-phase flows for turbulent mixing of sprays by means of two-phase PIV', *Experiments in Fluids* **39**, 895-908.

Kosiwczuk, W. (2006), 'Mesure simultanée des vitesses des gouttes et du gaz en mélange diphasique par PIV et fluorescence', PhD thesis, Université de Rouen.

Lecordier, B. (1997), 'Etude de l'interaction de la propagation d'une flamme prémélangée avec le champ aérodynamique, par association de la tomographie laser et de la vélocimétrie par images de particules', PhD thesis, Université de Rouen.

Prosperi, B. (2008), 'Analyse de l'entraînement d'air induit par le développement instationnaire d'un spray conique creux. Application à l'injection directe essence.', PhD thesis, INP Toulouse.